

# Reduction of quantization noise via periodic code for oversampled input signals and the corresponding optimal code design



Bingo Wing-Kuen Ling<sup>a,\*</sup>, Charlotte Yuk-Fan Ho<sup>b,1</sup>, Qingyun Dai<sup>a,2</sup>,  
Joshua D. Reiss<sup>c,3</sup>

<sup>a</sup> Faculty of Information Engineering, Guangdong University of Technology, Guangzhou 510006, China

<sup>b</sup> Department of Electronic and Information Engineering, The Hong Kong Polytechnic University, Hong Kong, China

<sup>c</sup> Department of Electronic Engineering, Queen Mary University of London, Mile End Road, London, E1 4NS, United Kingdom

## ARTICLE INFO

### Article history:

Available online 16 October 2013

### Keywords:

Reduction of quantization noise  
Oversampled signals  
Deterministic quantization model in frequency domain  
Semi-infinite programming  
Optimal design of periodic code  
Modified gradient descent method

## ABSTRACT

This paper proposes to reduce the quantization noise using a periodic code, derives a condition for achieving an improvement on the signal to noise ratio (SNR) performance, and proposes an optimal design for the periodic code. To reduce the quantization noise, oversampled input signals are first multiplied by the periodic code and then quantized via a quantizer. The signals are reconstructed via multiplying the quantized signals by the same periodic code and then passing through an ideal lowpass filter. To derive the condition for achieving an improvement on the SNR performance, first the quantization operator is modeled by a deterministic polynomial function. The coefficients in the polynomial function are defined in such a way that the total energy difference between the quantization function and the polynomial function is minimized subject to a specification on the upper bound of the absolute difference. This problem is actually a semi-infinite programming problem and our recently proposed dual parameterization method is employed for finding the globally optimal solution. Second, the condition for improving the SNR performance is derived via a frequency domain formulation. To optimally design the periodic code such that the SNR performance is maximized, a modified gradient descent method that can avoid the obtained solution to be trapped in a locally optimal point and guarantee its convergence is proposed. Computer numerical simulation results show that the proposed system could achieve a significant improvement compared to existing systems such as the conventional system without multiplying to the periodic code, the system with an additive dithering and a first order sigma delta modulator.

© 2013 Elsevier Inc. All rights reserved.

## 1. Introduction

Quantization is widely employed in many signal processing systems, such as in data compression [1] and analog to digital conversion [2] systems. However, as the quantization is not a reversible process because it is a many to one mapping, signals cannot be perfectly reconstructed after the quantization [3]. As a result, efficient methods for the reduction of the quantization noise are very useful for many signal processing applications.

The most common method to minimize the quantization noise is to perform the quantization based on the statistics of input signals [4]. Finer resolutions are assigned to the ranges of input

signals which occur most frequently, and vice versa. However, this kind of quantization schemes requires a prior knowledge of the statistics of input signals. In many situations, the statistics of input signals are unknown and this method cannot be applied directly.

Dithering is also a common method for reducing the quantization noises. However, it worth noting that there are two main fundamental differences between the system with an additive dithering and the proposed system. First, in the system with an additive dithering, a white noise is added and subtracted before and after the quantizer, respectively. On the other hand, a periodic code is multiplied before and after the quantizer in the proposed system. Just changing addition to multiplication will require a very different analytical technique and come up to a very different result. Statistical analysis of an additive noise can be performed easily and plenty of the existing results can be applied. However, the existing techniques for analyzing multiplicative noise are limited and this problem is theoretically challenging. Second, the introduced noise in the additive dithering approach is a random process, while the periodic code in the proposed system is a deterministic signal.

\* Corresponding author. Fax: +86 20 3932 2252.

E-mail addresses: yongquanling@gdut.edu.cn (B.W.-K. Ling), c.ho@eie.polyu.edu.hk (C.Y.-F. Ho), daiqy@gdut.edu.cn (Q. Dai), josh.reiss@elec.qmul.ac.uk (J.D. Reiss).

<sup>1</sup> Fax: +852 2362 84397.

<sup>2</sup> Fax: +86 20 3932 2025.

<sup>3</sup> Fax: +44 (0) 20 78827997.

Since these two signals are very different in nature, the analysis of these two systems is also very different. In terms of the computational effort and the cost of an implementation, since the implementation of the system with an additive dithering requires a random sequence, it is in general more difficult and costly. This is because it is very difficult and costly to generate a truly random signal with a uniform distribution. On the other hand, since a simple potential divider can be employed for performing the multiplication of signals, the implementation of the proposed system is easier and cheaper compared to the existing ones because the periodic code can be stored in memory and only multiplications are required.

Another approach similar to the dithering is via multiplying the signals before and after the quantization by a pseudorandom binary sequence. However, this method is also different from our proposed method. First, the pseudorandom signal is not optimally designed. On the other hand, the proposed periodic code is optimally designed. Second, the pseudorandom signal is only represented by one bit, while our proposed periodic code is represented by more than one bit. Hence, performances of our proposed system are better than those with multiplying the signals before and after the quantization by a pseudorandom binary sequence.

Sigma delta modulation is also widely used to minimize the quantization noise [2,3,5–7,10,11]. If input signals are oversampled, then the signals are bandlimited within a very narrow band [8]. By a proper design of the loop filter, the quantization noise can be further shaped away from the signal band. Although this method can sometimes achieve very high SNRs, many high order sigma delta modulators suffer from the instability problem particularly when the input magnitudes are close to the saturation level of the quantizer [12–14].

In order to reduce the quantization noise with the guarantee of the stability without the prior knowledge on the statistics of input signals, this paper proposes to multiply signals before and after the quantization by a periodic code. Here, the periodic code means a periodic sequence. Periodic codes are widely employed in spread spectrum communication systems. The motivation of the use of the periodic code is based on the fact that the conventional system without multiplying by the periodic code is actually a particular case of the proposed system when the periodic code is equal to one and the period of the code is also equal to one. Hence, the proposed system is the generalization of the conventional system and should achieve an improvement on the signal to noise (SNR) ratio performance if the periodic code is designed properly. The working principles of the proposed method are based on the following arguments. A periodic code can be represented using the Fourier series. Multiplying the input signals by the periodic code is equivalent to the weighted sums of the input signals modulated at different harmonic frequencies. If the quantization operator can be modeled by a polynomial function, then the quantizer performs the weighted sums of the multiplications of the coded signals in the time domain. In the frequency domain, the quantizer performs the weighted sums of the convolutions of the coded signals. It is worth noting that the convolutions of the modulated components will result to the signal components with wider bandwidths and shifting their center frequencies to other harmonic frequencies. After multiplying the quantized signals by the same periodic code and passing through a lowpass filter, all signal components centered at the higher harmonic frequencies will be discarded and only the base band signal component is retained. Although aliasing still occurs in the base band, the effect of the aliasing due to these higher order terms in the polynomial can be minimized by a proper design of the periodic code.

In this paper, the input signal is assumed to be oversampled and it is in the discrete time form. Instead of investigating the analog to digital and digital to analog conversions, this paper is

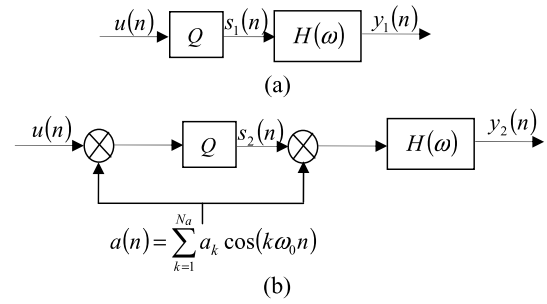


Fig. 1. (a) Conventional system. (b) Proposed system with a periodic code.

to reduce the quantization noise in such a way that the stability of the system is guaranteed without the prior knowledge on the statistics of input signals. To achieve this goal, this paper proposes to multiply the signals before and after the quantization by a periodic code. The outline of this paper is as follow. In Section 2, an approximated model for the quantizer is introduced. Based on the approximated model, detail noise analysis including the derivation of a condition for achieving an improvement on the SNR performance is presented in Section 3. In Section 4, a modified gradient descent method is proposed for designing a periodic code such that the SNR performance is maximized. The proposed method can avoid the obtained solution to be trapped in a locally optimal point and guarantee the convergence of the proposed algorithm. In Section 5, numerical computer simulation results are presented. Finally, a conclusion is drawn in Section 6.

## 2. Approximated quantization model

It is assumed in many quantization systems that the quantization noise is modeled by an additive wide sense stationary white noise source. The input of the quantizer is also assumed to be a stationary random process. Each sample of the quantization error is assumed to be uniformly distributed over the range of the quantization step size and uncorrelated to the input of the quantizer. Recently, the histogram of the quantizer output is derived analytically based on nonlinear system theories [10]. This result verifies that the assumptions made in the conventional system are invalid and far from practical situations especially for low bit quantizer cases [10]. Hence, a deterministic model, instead of a statistical model, is proposed in this paper.

The block diagrams of a conventional system and the proposed system are shown in, respectively, Fig. 1a and Fig. 1b. Denote the input of these two systems, the quantizer, the frequency response of the linear time invariant filter, the output of the conventional quantizer, the output of the quantizer of the proposed system, the output of the conventional system and the output of the proposed system as, respectively,  $u(n)$ ,  $Q(\cdot)$ ,  $H(\omega)$ ,  $s_1(n)$ ,  $s_2(n)$ ,  $y_1(n)$  and  $y_2(n)$ . We assume that  $u(n)$  is oversampled. That means,  $u(n)$  is bandlimited within the frequency spectrum  $(-\frac{\pi}{R}, \frac{\pi}{R})$ , where  $R$  is the oversampling ratio (OSR). We also assume that  $H(\omega)$  is an ideal lowpass filter. That is,

$$H(\omega) = \begin{cases} 1 & |\omega| < \frac{\pi}{R}, \\ 0 & \text{otherwise.} \end{cases}$$

Consider an  $N$  bit uniform antisymmetric quantizer with the quantization range  $[-L, L]$ . That is,

$$Q(\mu(n)) \equiv \begin{cases} \Delta \text{sign}(\mu(n))(\text{ceil}(\frac{|\mu(n)|}{\Delta}) - \frac{1}{2}) & |\mu(n)| \leq L, \\ \text{sign}(\mu(n))L & |\mu(n)| > L, \end{cases} \quad (1)$$

where  $\mu(n)$  is the input of the quantizer,

$$\text{sign}(\mu(n)) \equiv \begin{cases} \frac{\mu(n)}{|\mu(n)|} & \mu(n) \neq 0, \\ 0 & \mu(n) = 0, \end{cases}$$

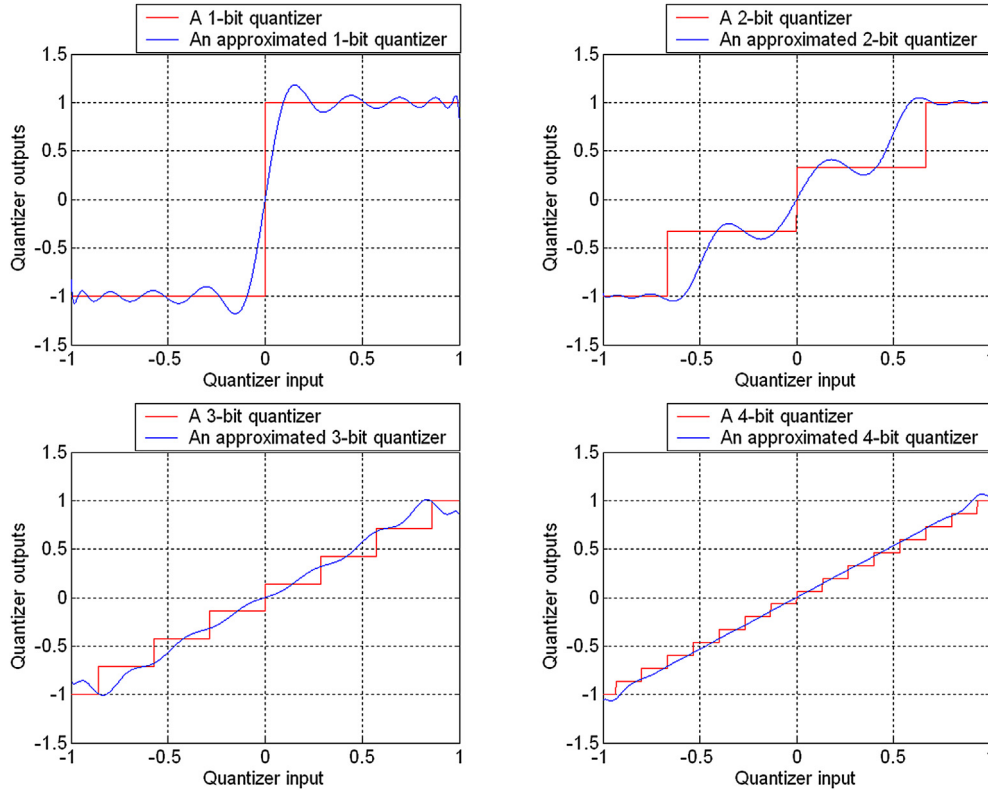


**Fig. 2.** Input output relationships of actual quantizers with  $L = 1$  and the approximated quantizers  $\mu^T(n)\mathbf{p}$  with  $M = 10$  for (a)  $N = 1$  bit, (b)  $N = 2$  bit, (c)  $N = 3$  bit and (d)  $N = 4$  bit.

$\text{ceil}(\mu(n))$  denotes the rounding operator towards the plus infinity,  $|\cdot|$  denotes the absolute operator, and  $\Delta \equiv \frac{L}{2^{N-1}-0.5}$  is the step size of the quantizer. Since the quantizer is characterized by a discontinuous nonlinearity, the overall system is very difficult to be analyzed. In order to analyze the overall system,  $Q(\mu(n))$  is approximated by a polynomial of  $\mu(n)$ . Denote  $\boldsymbol{\mu}(n) \equiv [\mu(n) \ (\mu(n))^3 \ \dots \ (\mu(n))^{2M-1}]^T$  and  $\mathbf{p} \equiv [p_1 \ \dots \ p_M]^T$ , where the superscript  $T$  denotes the transposition operator,  $p_m \in \Re$  for  $m = 1, 2, \dots, M$  and  $2M - 1$  are, respectively, the coefficients and the order of the polynomial, in which  $\Re$  denotes the set of real valued numbers. Since all the coefficients of the model are real valued, the proposed nonlinear model is a real valued system.  $\mathbf{p}$  can be found via minimizing the total energy difference between the quantization function and the polynomial function subject to a specification on the upper bound of the absolute difference. This is actually a semi-infinite programming problem. Define the specification on the upper bound as  $\frac{\varepsilon\Delta}{2}$ , where  $\varepsilon > 0$ . Then, the semi-infinite programming problem can be expressed as follow:

$$\min_{\mathbf{p}} \int_{-L}^L |\boldsymbol{\mu}^T(n)\mathbf{p} - Q(\mu(n))|^2 d\mu(n), \quad (2a)$$

$$\text{subject to } |\boldsymbol{\mu}^T(n)\mathbf{p} - Q(\mu(n))| \leq \frac{\varepsilon\Delta}{2} \quad \forall \mu(n) \in [-L, L], \quad (2b)$$

and can be solved via the dual parameterization method [7]. Fig. 2 shows examples of input–output relationships of actual quantizers with  $L = 1$  and the approximated quantizers  $\boldsymbol{\mu}^T(n)\mathbf{p}$  with  $M = 10$  for  $N = 1$  bit,  $N = 2$  bit,  $N = 3$  bit and  $N = 4$  bit. Fig. 3 shows the corresponding differences, that is  $Q(\mu(n)) - \boldsymbol{\mu}^T(n)\mathbf{p}$ . It can be seen from Fig. 2 that the solutions of the semi-infinite programming problems exist for  $N = 1, 2, 3, 4$  bit when  $M = 10$ .

It is worth noting that when the number of bits of quantizer increases, the accuracy of the model decreases if  $M$  remains un-

changed. However, as the coefficients of the model are the solution of the semi-infinite programming problem, if the solution of the semi-infinite programming problem exists, then the maximum absolute quantization error is guaranteed to be bounded by a constant ( $\frac{\varepsilon}{2}$ ) multiplying by the quantization step. Or in other words, the ratio of the maximum absolute quantization error to the quantization step is bounded by  $\frac{\varepsilon}{2}$  whenever the solution of the semi-infinite programming problem exists. For  $N = 1$  bit, the discontinuity point of the actual quantizer is at the origin. If the magnitude of input signals is small and the linear model is applied, then the difference between the output of the actual quantizer and that based on the linear model will be very large. Hence, a linear model is not appropriate for the approximation of low bit quantizers. For high bit quantizers, according to the results shown in Fig. 3, there are large errors and these large errors occur at the neighborhood of discontinuity points of the actual quantizer. To suppress these large errors, large values of  $M$  should be employed instead. Hence, a linear model is also not appropriate for the approximation of high bit quantizers. In Fig. 3, we use the same value of  $M$  for the illustration. This is because too large value of  $M$  would increase the total number of terms in the model and hence increase the computational effort for the design of the periodic code. The details will be explained in the next section.

### 3. Noise analysis

Now, let's analyze the quantization noise using the approximated model discussed in the previous section. That is, replace the actual quantizer  $Q(\mu(n))$  by the approximated quantizer  $\boldsymbol{\mu}^T(n)\mathbf{p}$ . Denote the discrete time Fourier transform of  $u(n)$ ,  $s_1(n)$ ,  $s_2(n)$ ,  $y_1(n)$  and  $y_2(n)$  as, respectively,  $U(\omega)$ ,  $S_1(\omega)$ ,  $S_2(\omega)$ ,  $Y_1(\omega)$  and  $Y_2(\omega)$ . Let the periodic code be  $a(n)$ . Suppose that the periodic code is real valued, symmetric and with zero DC gain. Let its Fourier coefficients expressed in the cosine form be  $a_k$ . Note that a

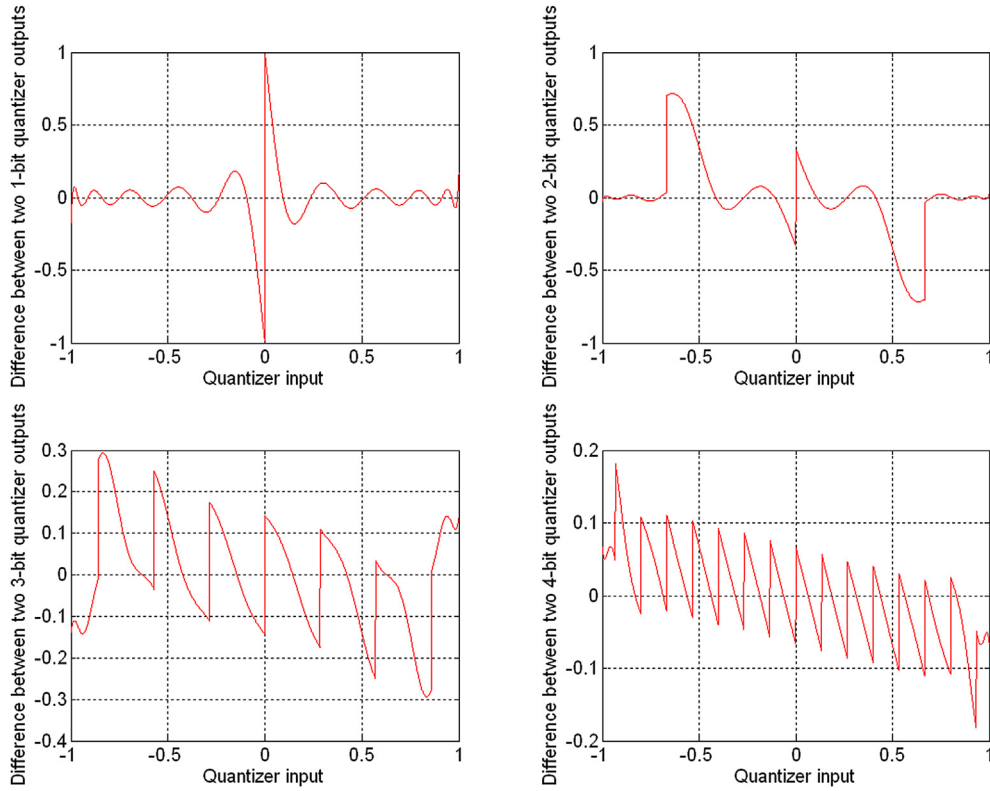


**Fig. 3.** The differences between the actual quantizers with  $L = 1$  and the approximated quantizers  $\mu^T(n)\mathbf{p}$  with  $M = 10$  for (a)  $N = 1$  bit, (b)  $N = 2$  bit, (c)  $N = 3$  bit and (d)  $N = 4$  bit.

real valued symmetric code can guarantee that  $a_k$  are real valued. This property facilitates the design of the code. Denote the length of the code as  $2N_a + 1$ . Denote the fundamental frequency of the periodic code as  $\omega_0 \equiv \frac{2\pi}{2N_a+1}$ . Then,  $a(n) \equiv \sum_{k=1}^{N_a} a_k \cos(k\omega_0 n)$ . Define  $\tilde{A}(\omega) \equiv \sum_{k=1}^{N_a} a_k \pi (\delta(\omega - k\omega_0) + \delta(\omega + k\omega_0))$ ,  $U_{2m-1}(\omega) \equiv U(\omega) * \dots * U(\omega)$  and  $\tilde{A}_{2m-1}(\omega) \equiv \tilde{A}(\omega) * \dots * \tilde{A}(\omega)$ , where  $*$  denotes the convolution operator. Here, the convolution operator is defined as  $P(\omega) * Q(\omega) \equiv \frac{1}{2\pi} \int_{-\pi}^{\pi} P(\theta) * Q(\omega - \theta) d\theta$ , and there are  $2m - 1$  terms in both  $U_{2m-1}(\omega)$  and  $\tilde{A}_{2m-1}(\omega)$ . Define  $\mathbf{a} \equiv \pi [a_1 \dots a_{N_a}]^T$  and  $\tilde{\mathbf{a}}_m \equiv [\text{fliplr}(\mathbf{a}^T) \ 0 \ \mathbf{a}^T]^T$ , where  $\text{fliplr}(\mathbf{a}^T) \equiv [a_{N_a} \dots a_1]$ .  $\tilde{\mathbf{a}}_m$  is a vector representing the coefficients of  $\tilde{A}(\omega)$  at different harmonics. Let the discrete Fourier transform of  $\tilde{\mathbf{a}}_m$  be  $\hat{\mathbf{a}}_m$  and its  $k$ th element be  $\hat{a}_m(k)$ . Denote a vector  $\tilde{\mathbf{a}}_m$  with the  $k$ th element denoted as  $\tilde{a}_m(k)$ . Here,  $\tilde{a}_m(k)$  is defined as  $\tilde{a}_m(k) \equiv (\hat{a}_m(k))^{2m}$ . Let the inverse discrete Fourier transform of  $\tilde{\mathbf{a}}_m$  be  $\mathbf{a}'_m$  and the  $k$ th element be  $a'_m(k)$ . Obviously,  $\mathbf{a}'_m$  is a vector representing the coefficients of  $\tilde{A}_{2m}(\omega)$  at different harmonics. Define  $a''_m \equiv a'_m(N_a + 1)$ .

**Theorem 1.** Assume that  $Q(\mu(n)) \approx \mu^T(n)\mathbf{p}$ ,

$$H(\omega) = \begin{cases} 1 & |\omega| < \frac{\pi}{R}, \\ 0 & \text{otherwise,} \end{cases}$$

$\omega_0 \geq \frac{2\pi(2M-1)}{R}$  and  $(2 \sum_{k=1}^{N_a} \frac{a_k^2}{4})^2 \int_{-\frac{\pi}{R}}^{\frac{\pi}{R}} |\sum_{m=2}^M p_m U_{2m-1}(\omega)|^2 d\omega > \int_{-\frac{\pi}{R}}^{\frac{\pi}{R}} |\sum_{m=2}^M p_m a''_m U_{2m-1}(\omega)|^2 d\omega$ . Then, the SNR of the coded system shown in Fig. 1b will be higher than that of the conventional system shown in Fig. 1a.

**Proof.** If  $Q(\mu(n)) \approx \mu^T(n)\mathbf{p}$ , then we have

$$Y_1(\omega) = H(\omega)S_1(\omega) \approx H(\omega) \sum_{m=1}^M p_m U_{2m-1}(\omega) \quad (3)$$

for the conventional system shown in Fig. 1a. If we regard the first order term ( $m = 1$ ) in the signal band as the signal component and all higher order terms ( $m \geq 2$ ) in the signal band as the quantization noise, then the SNR can be estimated as follows:

$$\text{SNR} \approx 10 \log_{10} \frac{\int_{-\frac{\pi}{R}}^{\frac{\pi}{R}} |H(\omega)p_1 U(\omega)|^2 d\omega}{\int_{-\frac{\pi}{R}}^{\frac{\pi}{R}} |H(\omega) \sum_{m=2}^M p_m U_{2m-1}(\omega)|^2 d\omega}. \quad (4a)$$

Since  $H(\omega)$  is an ideal lowpass filter, we have:

$$\text{SNR} \approx 10 \log_{10} \frac{p_1^2 \int_{-\frac{\pi}{R}}^{\frac{\pi}{R}} |U(\omega)|^2 d\omega}{\int_{-\frac{\pi}{R}}^{\frac{\pi}{R}} |\sum_{m=2}^M p_m U_{2m-1}(\omega)|^2 d\omega}. \quad (4b)$$

Now consider the coded system shown in Fig. 1b. Denote the input to the quantizer as  $\tilde{u}(n)$  and define  $\tilde{U}_{2m-1}(\omega) \equiv \tilde{U}(\omega) * \dots * \tilde{U}(\omega)$ , where there are  $2m - 1$  terms in  $\tilde{U}_{2m-1}(\omega)$ . Since  $\tilde{U}(\omega) = U(\omega) * \tilde{A}(\omega)$ , we have  $\tilde{U}_{2m-1}(\omega) = U_{2m-1}(\omega) * \tilde{A}_{2m-1}(\omega)$ . As we assume that  $Q(\mu(n)) \approx \mu^T(n)\mathbf{p}$ , we have  $S_2(\omega) \approx \sum_{m=1}^M p_m U_{2m-1}(\omega) * \tilde{A}_{2m-1}(\omega)$  and

$$Y_2(\omega) \approx H(\omega) \sum_{m=1}^M p_m U_{2m-1}(\omega) * \tilde{A}_{2m}(\omega). \quad (5)$$

As a result, we have:

$$\text{SNR} \approx 10 \log_{10} \frac{\int_{-\frac{\pi}{R}}^{\frac{\pi}{R}} |H(\omega)p_1 U(\omega) * \tilde{A}_2(\omega)|^2 d\omega}{\int_{-\frac{\pi}{R}}^{\frac{\pi}{R}} |H(\omega) \sum_{m=2}^M p_m U_{2m-1}(\omega) * \tilde{A}_{2m}(\omega)|^2 d\omega}. \quad (6a)$$

Since  $\omega_0 \geq \frac{2\pi(2M-1)}{R}$  and  $u(n)$  is bandlimited, the terms in  $U_{2m-1}(\omega) * \tilde{A}_{2m}(\omega)$  for  $m = 1, 2, \dots, M$  at different harmonics do

not overlap each others in the frequency spectrum. As  $H(\omega)$  is an ideal lowpass filter, (6a) can be further simplified as:

$$SNR \approx 10 \log_{10} \frac{p_1^2 (2 \sum_{k=1}^{N_a} \frac{a_k^2}{4})^2 \int_{-\frac{\pi}{R}}^{\frac{\pi}{R}} |U(\omega)|^2 d\omega}{\int_{-\frac{\pi}{R}}^{\frac{\pi}{R}} |H(\omega) \sum_{m=2}^M (p_m U_{2m-1}(\omega) * \tilde{A}_{2m}(\omega))|^2 d\omega} \quad (6b)$$

Since  $\omega_0 \geq \frac{2\pi(2M-1)}{R}$ ,  $u(n)$  is bandlimited and  $H(\omega)$  is an ideal lowpass filter, we have:

$$SNR \approx 10 \log_{10} \frac{p_1^2 (2 \sum_{k=1}^{N_a} \frac{a_k^2}{4})^2 \int_{-\frac{\pi}{R}}^{\frac{\pi}{R}} |U(\omega)|^2 d\omega}{\int_{-\frac{\pi}{R}}^{\frac{\pi}{R}} |\sum_{m=2}^M p_m a_m'' U_{2m-1}(\omega)|^2 d\omega} \quad (6c)$$

If

$$\left( 2 \sum_{k=1}^{N_a} \frac{a_k^2}{4} \right)^2 \int_{-\frac{\pi}{R}}^{\frac{\pi}{R}} \left| \sum_{m=2}^M p_m U_{2m-1}(\omega) \right|^2 d\omega > \int_{-\frac{\pi}{R}}^{\frac{\pi}{R}} \left| \sum_{m=2}^M p_m a_m'' U_{2m-1}(\omega) \right|^2 d\omega,$$

then the SNR of the coded system will be larger than that of the conventional system. This completes the proof. □

#### 4. Optimal periodic code design

In order to design an optimal code to maximize the SNR, a modified gradient descent method similar to that in [9] is proposed as follows:

##### Algorithm 1.

Step 1: Initialize iteration indices  $n = 0$  and  $t = 0$ . Generate a random vector  $\mathbf{a}^0$ , set  $l^0 = 0$ ,  $\lambda_0 = 1$ ,  $\tilde{N} = 1000$ ,  $\hat{N} = 10$  and  $\delta = \delta' = 10^{-6}$ . (These values are employed because they are typical for most gradient descent methods and global optimization algorithms.) Choose  $N_a = 40$  and  $M = 10$ . (The reasons for employing these values will be discussed in Section 5.)

Step 2: Assume that  $u(k) = U \sin(\frac{2\pi k}{3R})$ . (The reason for employing this input signal will also be discussed in Section 5.) Compute a new periodic code  $\mathbf{a}^{n+1} = \mathbf{a}^n - \lambda_n \nabla_{\mathbf{a}} SNR|_{\mathbf{a}=\mathbf{a}^n}$  and set  $\lambda_{n+1} = \frac{\lambda_0}{(\text{ceil}(\frac{n}{\tilde{N}}))^2}$ , where

$$\begin{aligned} \nabla_{a_k} SNR &= \frac{10}{\ln(10)} \left( \frac{a_k p_1^2 (2 \sum_{k=1}^{N_a} \frac{a_k^2}{4})^2 \int_{-\frac{\pi}{R}}^{\frac{\pi}{R}} |U(\omega)|^2 d\omega}{p_1^2 (2 \sum_{k=1}^{N_a} \frac{a_k^2}{4})^2 \int_{-\frac{\pi}{R}}^{\frac{\pi}{R}} |U(\omega)|^2 d\omega} \right. \\ &\quad - \left[ \int_{-\frac{\pi}{R}}^{\frac{\pi}{R}} (\nabla_{a_k} a_m'') \left( p_k U_{2k-1}(\omega) \sum_{m=2}^M p_m a_m'' U_{2m-1}^*(\omega) \right. \right. \\ &\quad \left. \left. + p_k U_{2k-1}^*(\omega) \sum_{m=2}^M p_m a_m'' U_{2m-1}(\omega) \right) d\omega \right] \\ &\quad \left. \times \left[ \int_{-\frac{\pi}{R}}^{\frac{\pi}{R}} \left| \sum_{m=2}^M p_m a_m'' U_{2m-1}(\omega) \right|^2 d\omega \right]^{-1} \right), \end{aligned}$$

$$\nabla_{\mathbf{a}} SNR \equiv [\nabla_{a_1} SNR \cdots \nabla_{a_{N_a}} SNR]^T$$

and

$$\begin{aligned} \nabla_{a_k} a_m'' &= \sum_{q=1}^{2N_a+1} 2m \tilde{W}_{N_a+1,q} \\ &\quad \times \left( \sum_{p=1}^{N_a} W_{q,p} a_{N_a+1-p} + W_{q,N_a+1+p} a_p \right) \\ &\quad \times (W_{q,N_a+1-k} + W_{q,N_a+1+k}), \end{aligned}$$

in which  $\mathbf{W}$  and  $\tilde{\mathbf{W}}$  are the discrete Fourier transform matrix and the inverse discrete Fourier transform matrix, respectively,  $W_{p,q}$  and  $\tilde{W}_{p,q}$  are the elements in the  $p$ th row and the  $q$ th column of  $\mathbf{W}$  and  $\tilde{\mathbf{W}}$ , respectively, and  $p_m$  for  $m = 1, 2, \dots, M$  are obtained via solving the corresponding semi-infinite programming problem [7].

Step 3: If  $|\mathbf{a}^{n+1} - \mathbf{a}^n| \leq \delta$ , then go to Step 4. Otherwise, increment the value of  $n$  and go to Step 2.

Step 4: Denote  $l^{t+1} = SNR|_{\mathbf{a}^{n+1}}$ . If  $0 < l^{t+1} - l^t \leq \delta'$  and  $t > \hat{N}$ , then take  $\mathbf{a}^{n+1}$  as the final approximated optimal solution. If  $l^{t+1} > l^t + \delta'$ , then increment both the values of  $n$  and  $t$ , set  $a_i^{n+1} = (1 + r_i^t) a_i^n$  where  $a_i^n$  is the  $i$ th element of  $\mathbf{a}^n$  and  $r_i^t$  is a random scalar with uniform distribution between  $[-0.5, 0.5]$ , and go to Step 2. If  $l^{t+1} < l^t$ , then set  $\mathbf{a}^{n+1}$  to the vector  $\mathbf{a}^p$  where the index  $p$  is the index of  $\mathbf{a}^p$  when calculating  $l^t$ . Then, add a random vector on it, increment both the values of  $n$  and  $t$ , and go to Step 2.

In general, the gradient descent method is prone to divergence and usually finds solutions that are only locally optimal. To avoid the obtained solution being trapped in the locally optimal solution, once an approximated locally optimal solution is found, a random vector is added on it so that it is kicked out from the approximated locally optimal solution and a new approximated locally optimal solution is found. If the SNR of the current approximated locally optimal solution is lower than that of the previous one, then the current approximated locally optimal solution is discarded, the code corresponding to the previous locally optimal solution is re-used but a random vector is added on it and re-iterates the above procedures. Since  $N_a$  is finite and the objective function is continuous differentiable, there are finite number of local minima. Also, as the obtained SNR is monotonic increasing, the proposed algorithm guarantees to converge to the globally optimal solution if the exact locally optimal solutions are found every time when Step 3 is quitted.

In general, the convergence of the gradient descent method would depend on  $\lambda_n$ . Small values of  $\lambda_n$  can guarantee the convergence and vice versa. In fact, both the accuracy of the obtained solution and the rate of the convergence are dependent on the values of  $\lambda_0$ ,  $\tilde{N}$ ,  $\delta$ ,  $\hat{N}$ ,  $r_i^t$  and  $\delta'$ . Small values of  $\delta$  and  $\lambda_n$  can reach the locally optimal solution with a high accuracy but with a slow rate of convergence, and vice versa. In this paper, large values of  $\lambda_n$  are employed in the early rounds of the iterations and vice versa so that the algorithm can reach a neighborhood of the locally optimal solution quickly and approach to the exact locally optimal solution slowly if the algorithm converges. In the case that the algorithm suffers from the divergence at the earlier stage, the value of  $\lambda_0$  should be re-chosen to a small value. In the case when the algorithm suffers from the divergence during the intermediate stage, the value of  $\tilde{N}$  should be re-chosen to a small value.

To kick out from the current locally optimal solution and reach another better locally optimal solution, a random vector is added to the current locally optimal solution. The location of the newly generated searching vector depends on  $r_i^t$ . If the value of  $r_i^t$  is chosen to be a small value, then the newly generated vector will

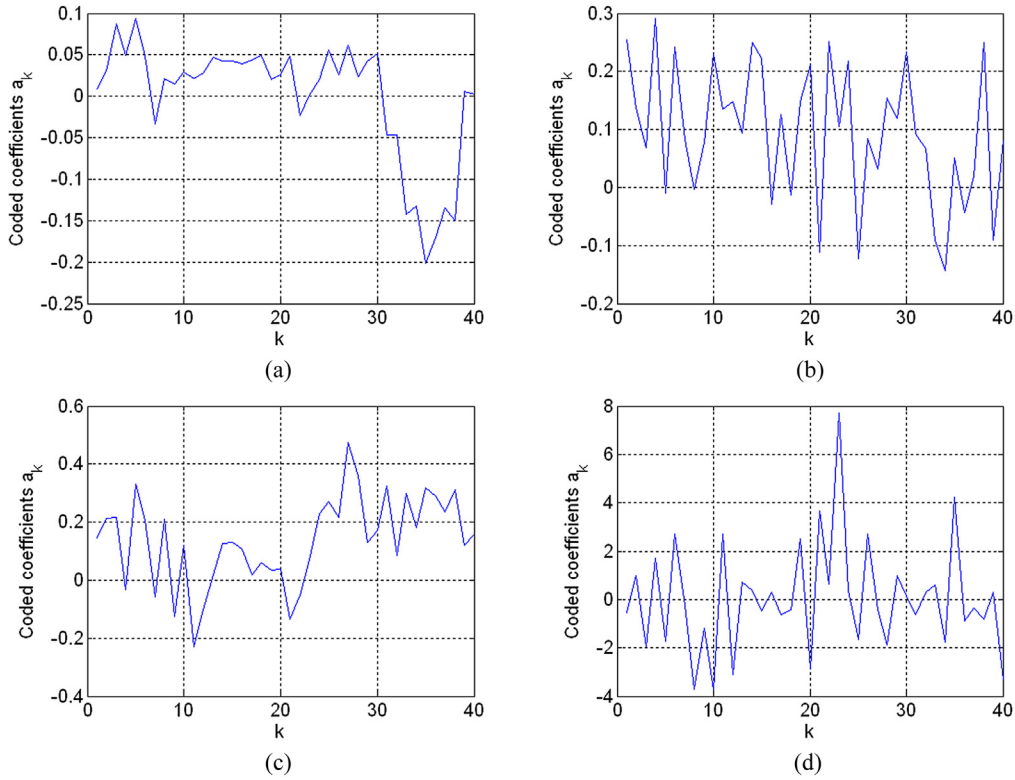


Fig. 4. Coefficients of the code when  $R = 32$  for (a)  $N = 1$  bit, (b)  $N = 2$  bit, (c)  $N = 3$  bit and (d)  $N = 4$  bit.

be close to the current locally optimal solution. In this case, the newly obtained locally optimal solution may be the same as the old one. Then, it requires an extra iteration step to kick out from the current locally optimal solution. This would increase the computational effort of the algorithm. However, if the value of  $r_i^t$  is chosen to be a large value, then the newly generated vector will move far away from the current locally optimal solution. In this case, some locally optimal solutions near the current locally optimal solution may be missed out. Hence, this paper chooses an intermediate value of  $r_i^t$  for the tradeoff reason. Also, the accuracy of the obtained solution and the rate of the convergence depend on both  $\hat{N}$  and  $\delta'$ . Small values of  $\delta'$  and large value of  $\hat{N}$  can improve the accuracy of the globally optimal solution but with a slow rate of convergence, and vice versa. In this paper, conventional values of  $\hat{N}$  and  $\delta'$  employed in general global optimization algorithms are chosen. Details are discussed in the next section.

## 5. Computer numerical simulation results

In this paper, the ideal lowpass filtering is implemented via computing the discrete Fourier transform of the signals, retaining the frequency components only within the frequency spectrum  $[-\frac{\pi}{R}, \frac{\pi}{R}]$  and computing the inverse discrete Fourier transform of the filtered signals. Sinusoidal signals are employed as test inputs because they are bandlimited within  $[-\frac{\pi}{R}, \frac{\pi}{R}]$ .

The following are the computer numerical simulation results of the periodic codes. The saturation level of the quantizer is chosen to be 1 due to the normalization reason. That is  $L = 1$ . The quantizers are the true quantizers with the discontinuous nonlinear functions. We choose  $N_a = 40$  and  $M = 10$ . These values are chosen because too large values of  $N_a$  and  $M$  would increase the computational effort. On the other hand, too small value of  $N_a$  and  $M$  limits the performance and cannot achieve good approximation model of the quantizer, respectively. The input is chosen as the normalized sum of sinusoidal signals defined as  $u(k) = \frac{\sum_{n=1}^{100} \sin(\frac{kn\pi}{100R})}{\max_{v_k \geq 0} (\sum_{n=1}^{100} \sin(\frac{kn\pi}{100R}))}$ .

By running Algorithm 1 at different number of bits of quantizers and different OSRs, the periodic codes are obtained and shown in Figs. 4 to 8. Since the coefficients of the approximate models are obtained via solving the corresponding semi-infinite programming problems, the coefficients of the approximated models for different number of bits of the quantizer are different even though the values of  $M$  are the same. Also, the thermal noise dominates as OSR increases. Hence, the obtained optimal periodic codes are different for different OSRs.

In terms of the performance analysis, it is worth noting that the proposed method would give worse results for large value of  $N$  when the numerical computer simulations are performed at the same value of  $M$ . This is because the number of terms of the polynomial required to approximate the quantizer should be increased as the number of bits of quantizer increases. As  $M$  remains unchanged, the accuracy of the approximated model decreases. However, if the value of  $M$  is increased, then the computational effort would increase. In order to tradeoff between the computational effort and the accuracy of the model, the same value  $M$  is employed in the computer numerical simulations. By running Algorithm 1 with the same input  $(u(k) = \frac{\sum_{n=1}^{100} \sin(\frac{kn\pi}{100R})}{\max_{v_k \geq 0} (\sum_{n=1}^{100} \sin(\frac{kn\pi}{100R}))})$ , the same quantizers (the quantizers are the true quantizers with the discontinuous nonlinear functions) with the same values of  $L$  ( $L = 1$ ), as well as at the same values of  $N_a$  ( $N_a = 40$ ) and  $M$  ( $M = 10$ ), Fig. 9 shows the improvements on the SNR performance for different number of bits of quantizers at different OSRs. It can be seen from Fig. 9 that the improvements on the SNR performance decreases as  $N$  increases. Fig. 10 shows the improvements on the SNR performance for different OSRs at different number of bits of quantizers. Since  $(2 \sum_{k=1}^{N_a} \frac{a_k^2}{4})^2 \int_{-\frac{\pi}{R}}^{\frac{\pi}{R}} |\sum_{m=2}^M p_m U_{2m-1}(\omega)|^2 d\omega - \int_{-\frac{\pi}{R}}^{\frac{\pi}{R}} |\sum_{m=2}^M p_m a_m'' U_{2m-1}(\omega)|^2 d\omega$  becomes smaller but the thermal noise becomes larger as OSR increases, it can be seen from Fig. 10

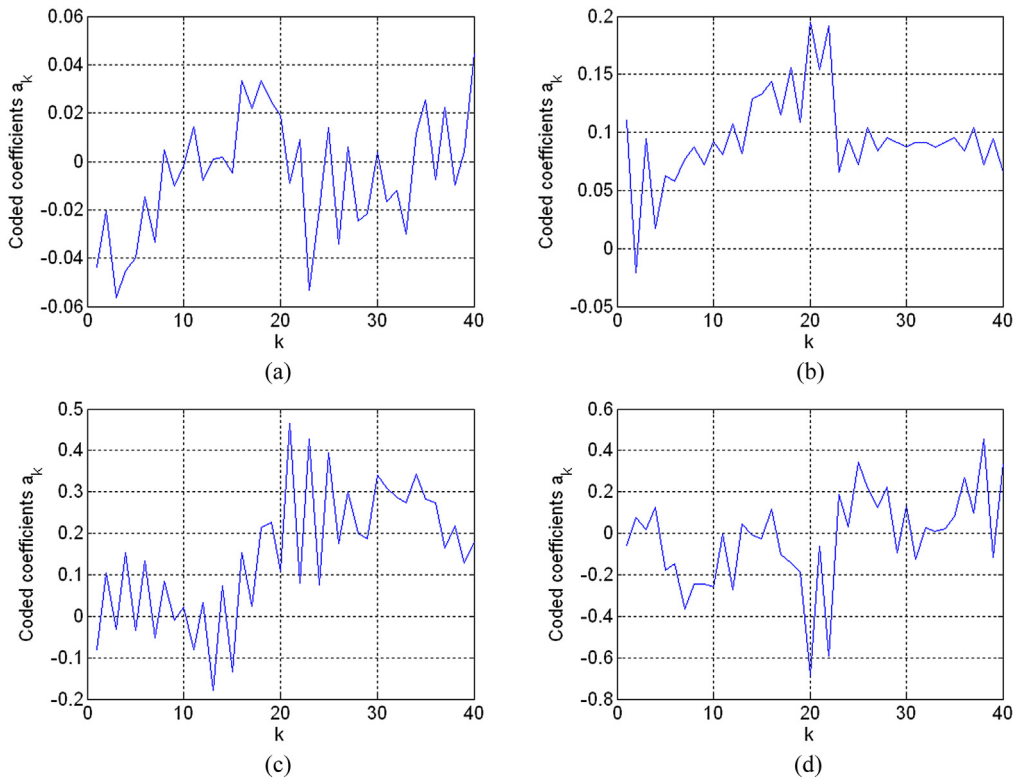


Fig. 5. Coefficients of the code when  $R = 64$  for (a)  $N = 1$  bit, (b)  $N = 2$  bit, (c)  $N = 3$  bit and (d)  $N = 4$  bit.

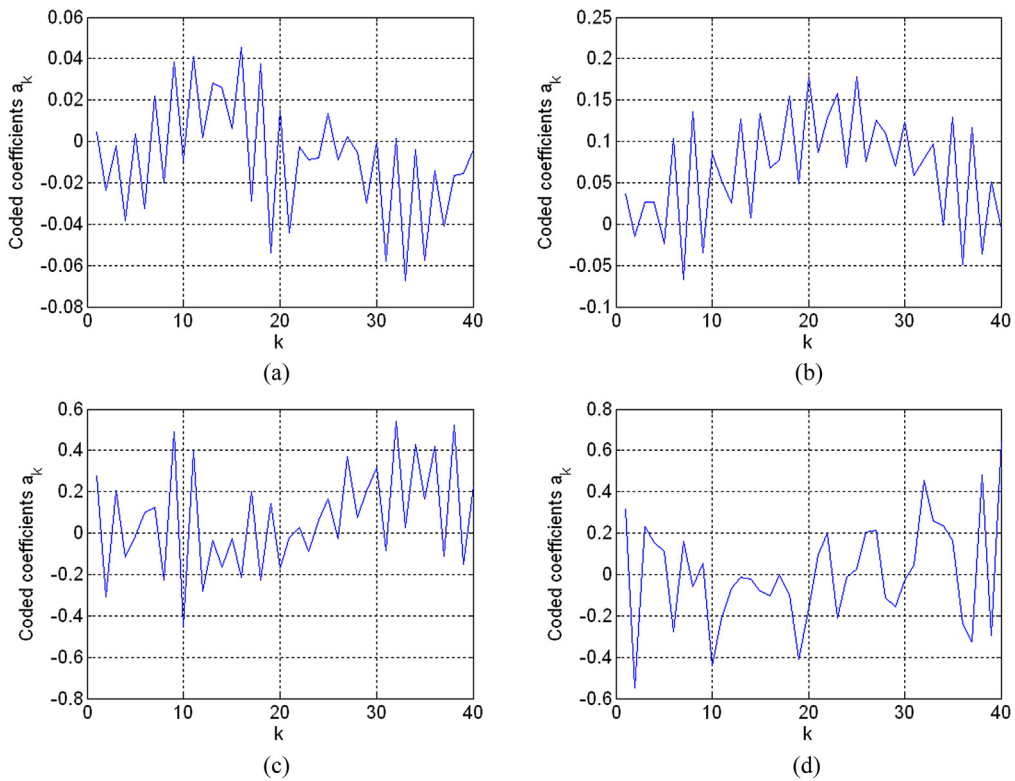


Fig. 6. Coefficients of the code when  $R = 128$  for (a)  $N = 1$  bit, (b)  $N = 2$  bit, (c)  $N = 3$  bit and (d)  $N = 4$  bit.

that there is no simple relationship between the improvements on the SNR performance and OSR.

To compare the performances of our proposed system, improvements on the SNR performance of the proposed system over the conventional system and the system with an additive dithering are

shown in Fig. 11. Here, an additive white noise source with a uniform distribution between  $[-1, 1]$  is added and subtracted before and after the quantizer in the system with an additive dithering, respectively. Since the less tones in the input signal will result to the less spurious tones but with higher magnitudes in the quan-

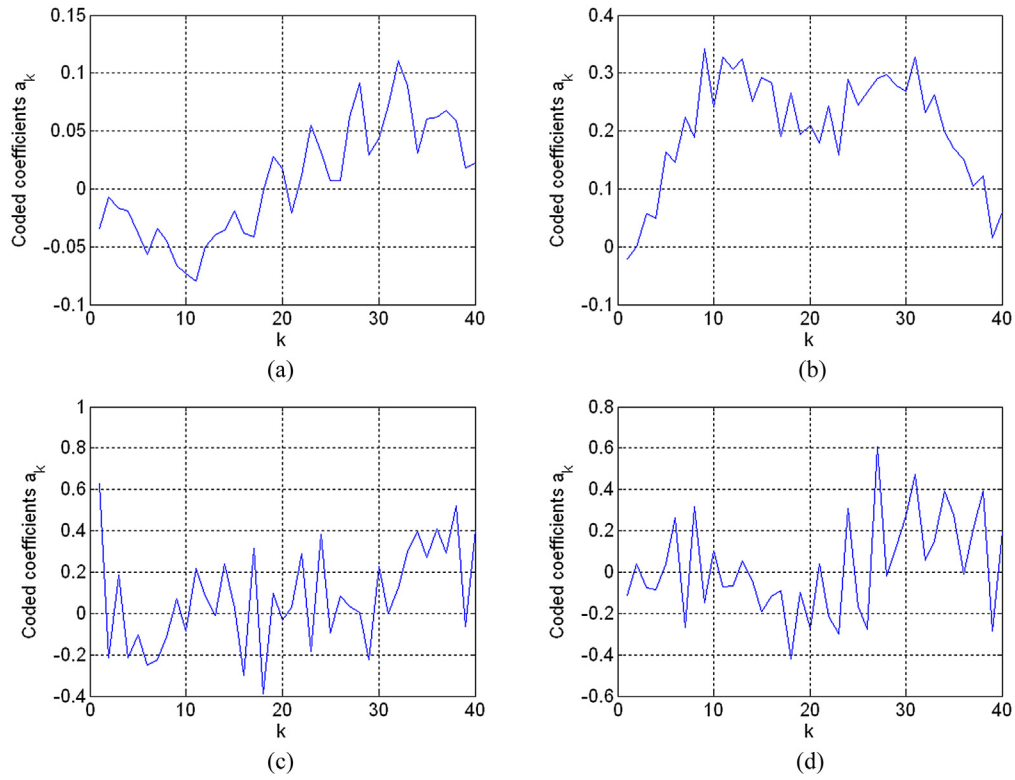


Fig. 7. Coefficients of the code when  $R = 256$  for (a)  $N = 1$  bit, (b)  $N = 2$  bit, (c)  $N = 3$  bit and (d)  $N = 4$  bit.

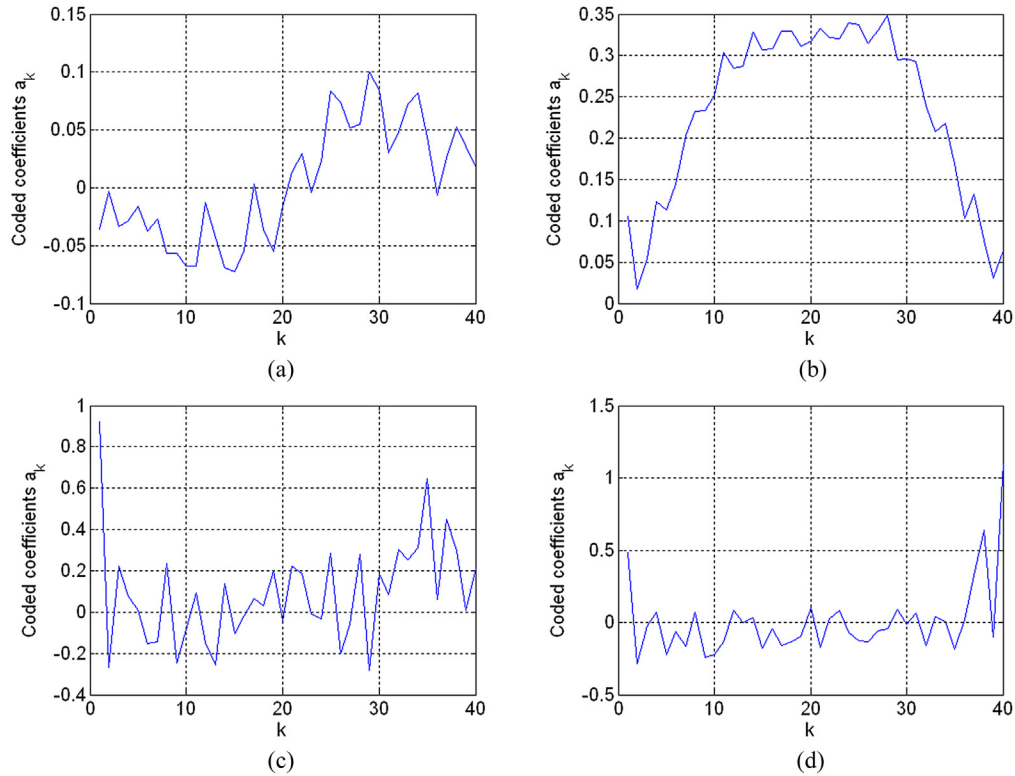


Fig. 8. Coefficients of the code when  $R = 512$  for (a)  $N = 1$  bit, (b)  $N = 2$  bit, (c)  $N = 3$  bit and (d)  $N = 4$  bit.

tizer output, we assume that the input signal is  $u(k) = U \sin(\frac{2\pi k}{3R})$  for  $k \geq 0$ . Here,  $U$  is the magnitude of the sinusoidal input. Since the thermal noise would be dominated when the OSR is very large, the comparison with very high OSR is not meaningful and  $R = 64$  is employed for the comparison. The quantizer is assumed to be

a single bit antisymmetric one with the saturation level equal to one. That is,

$$Q'(y) \equiv \begin{cases} 1 & y \geq 0, \\ -1 & \text{otherwise,} \end{cases}$$

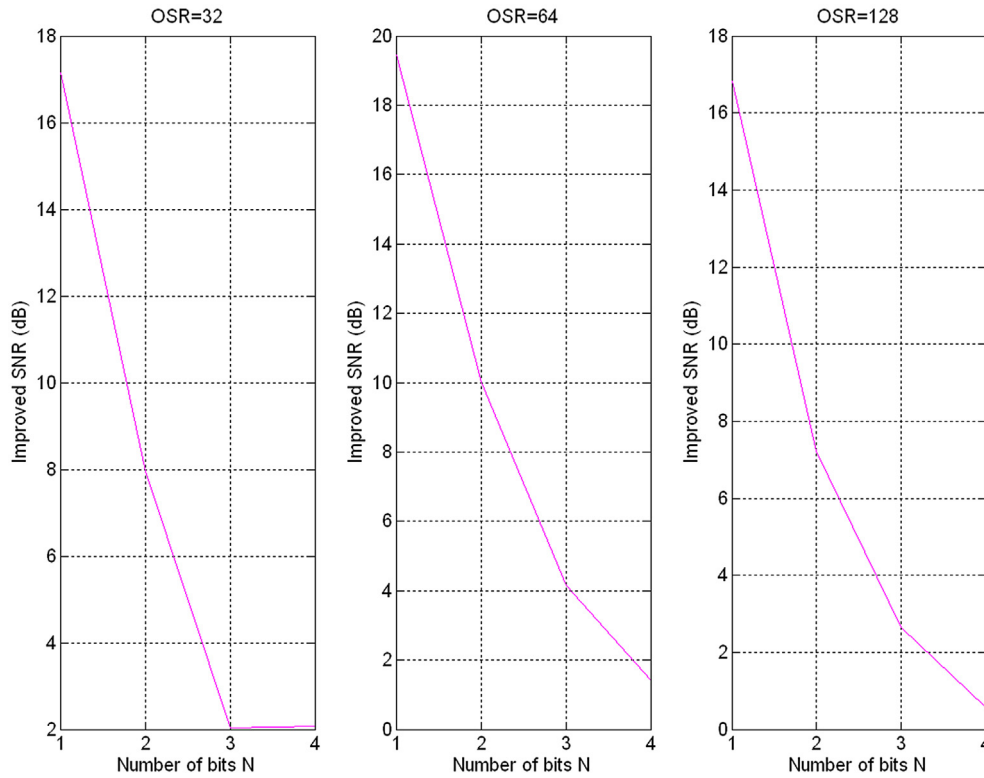


Fig. 9. Relationships between the improvements on the SNRs of the proposed system over the conventional system and the number of bits of quantizer when (a)  $R = 32$ , (b)  $R = 64$  and (c)  $R = 128$ .

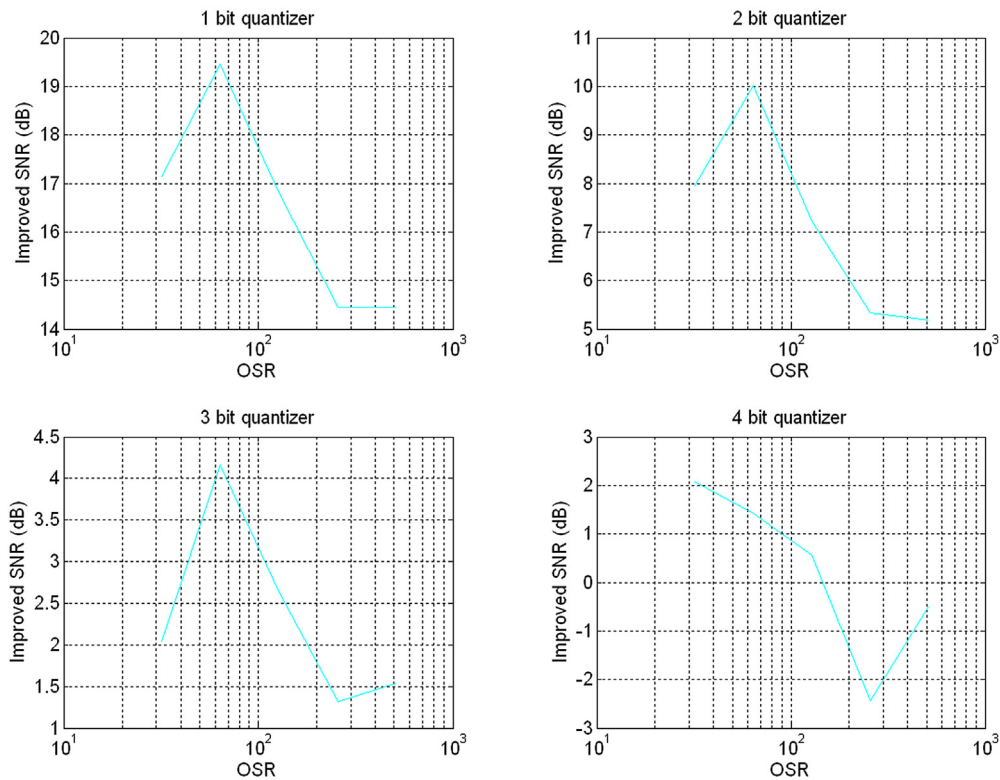


Fig. 10. Relationships between the improvements on the SNRs of the proposed system over the conventional system and the OSR when (a)  $N = 1$  bit, (b)  $N = 2$  bit, (c)  $N = 3$  bit and (d)  $N = 4$  bit.

and  $L = 1$ . This sinusoidal input and the quantizer are widely employed for the evaluation in industries. The periodic codes employed in these numerical computer simulations consist of 40 coefficients with  $M = 10$ .  $N_a = 40$  with  $M = 10$  is employed because

of similar reasons discussed before. According to the numerical computer simulation results, the proposed system could achieve an average of 101 dB improvement over the conventional system and an average of 85 dB improvement over the system with an

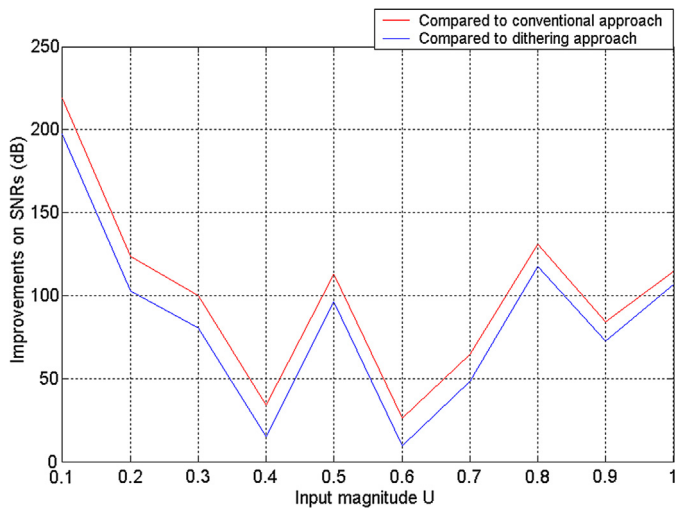


Fig. 11. Improvements on the SNR performance of the proposed system over the conventional system and the system with the additive dithering.

additive dithering. The proposed system achieves very significant improvements over the system with an additive dithering and the conventional system because the bandwidth of the input signal is zero as the discrete time Fourier transform of the input signal is the delta function. Hence, the overlap in the frequency domain after the convolution is minimal and very high SNR ratio can be achieved.

To compare the improvements on the SNR of the proposed system over a first order sigma delta modulator, the loop filter of the first order sigma delta modulator is realized via the state space matrices  $A = 1$ ,  $B = 1$ ,  $C = 1$  and  $D = 0$  and the zero initial condition is assumed to be zero. That is,  $x(0) = 0$ . A single bit antisymmetric quantizer with the saturation level equal to one, that is

$$Q'(y) \equiv \begin{cases} 1 & y \geq 0, \\ -1 & \text{otherwise,} \end{cases}$$

and  $L = 1$ , are employed for the illustration. The periodic code employed in this numerical computer simulation consists of 40 coefficients with  $M = 10.N_a = 40$  with  $M = 10$  is employed because of similar reasons discussed before. Consider the input signal

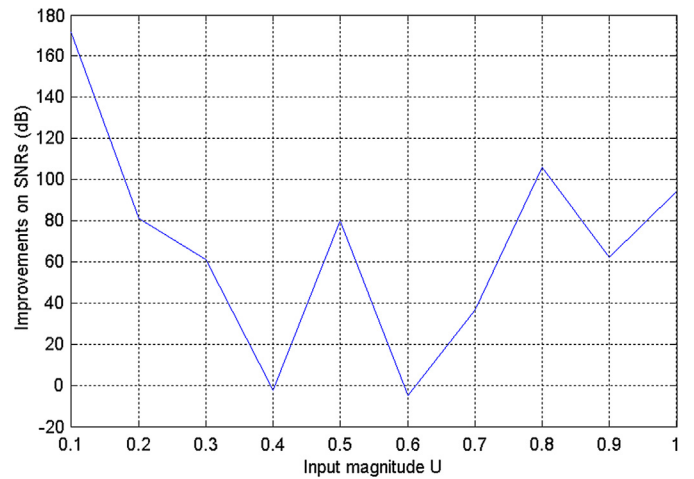


Fig. 12. Improvement on the SNR performance of the proposed system over a first order sigma delta modulator.

$u(k) = U \sin(\frac{2\pi k}{3R})$  for  $k \geq 0$ , where  $R = 64$  and  $U$  is the magnitude of the sinusoidal input. This input signal, OSR and the first order loop filter are employed for an illustration because of the similar reasons discussed in the above. It is worth noting that this first order sigma delta modulator is not BIBO stable. This is because there is a DC pole on the unit circle. The improvement on the SNR performance of the proposed system over this first order sigma delta modulator is shown in Fig. 12. It can be seen from Fig. 12 that the proposed system achieves an average of 69 dB improvement over this first order sigma delta modulator.

To test the robustness of the proposed method, variations on the quantization levels, inputs with DC offsets and finite word length effects on the periodic codes are considered. Since quantization levels are never exact in practical situations, improvements on the SNR performance of the proposed system over the conventional system and the system with an additive dithering for nonexact quantization level cases are shown in Fig. 13. Similar to the above, an additive white noise source with a uniform distribution between  $[-1, 1]$  is added and subtracted before and after the quantizer in the system with an additive dithering, respectively. Same as the above, we assume that the input signal is  $u(k) = U \sin(\frac{2\pi k}{3R})$  for  $k \geq 0$ , where  $R = 64$  and  $U$  is the magnitude

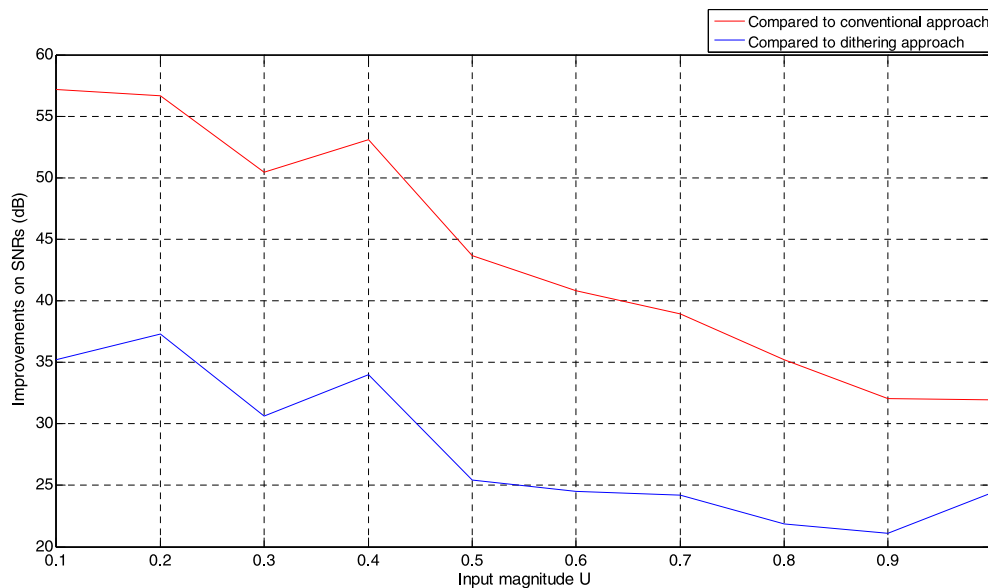


Fig. 13. Improvements on the SNR performance of the proposed system over the conventional system and the system with the additive dithering when  $L = 0.99$ .

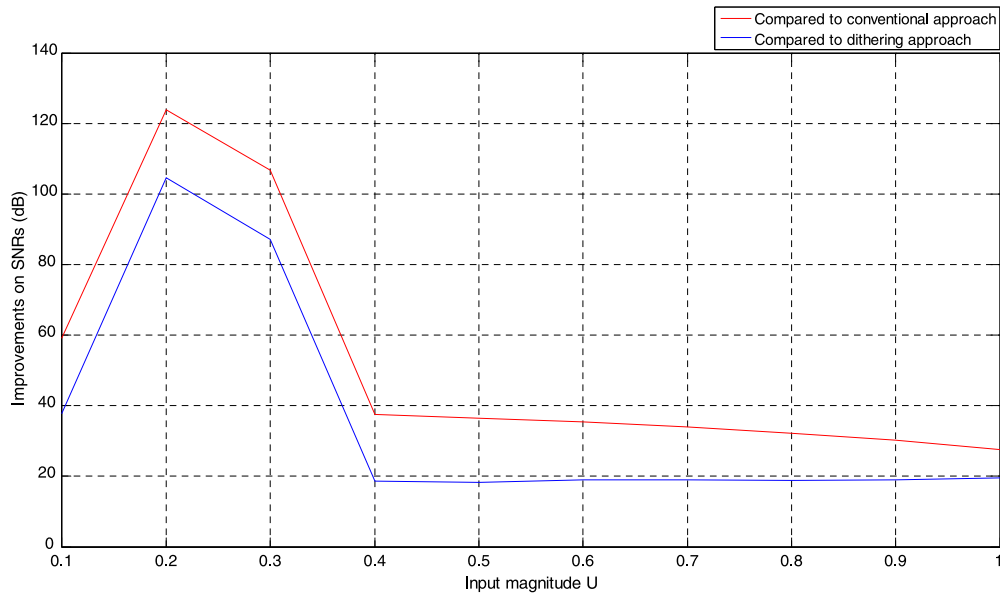


Fig. 14. Improvements on the SNR performance of the proposed system over the conventional system and the system with the additive dithering when the input signal has 0.01 DC offset.

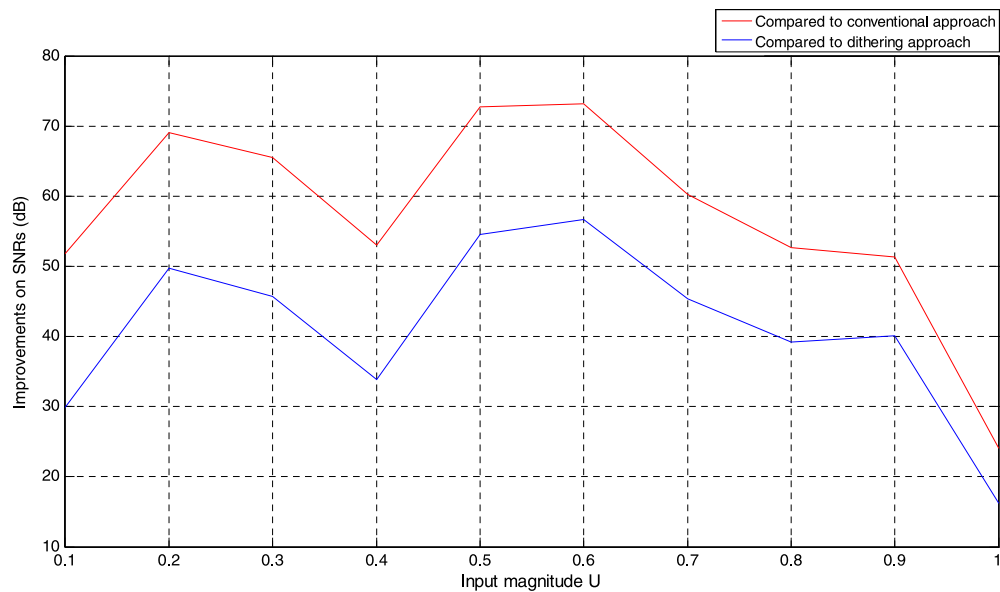


Fig. 15. Improvements on the SNR performance of the proposed system over the conventional system and the system with the additive dithering when the periodic code is represented using an 8 bit length.

of the sinusoidal input. The quantizer is assumed to be a single bit antisymmetric one with the saturation level equal to 0.99. That is

$$Q'(y) \equiv \begin{cases} 0.99 & y \geq 0, \\ -0.99 & \text{otherwise.} \end{cases}$$

The periodic codes employed in these numerical computer simulations consist of 40 coefficients with  $M = 10$ . According to the numerical computer simulation results, the proposed system could achieve an average of 44 dB improvement over the conventional system and an average of 27.8637 dB improvement over the system with an additive dithering. Although there are drops in terms of the improvements, the proposed system still achieves very significant improvements over the system with an additive dithering and the conventional system when the quantizer is not exact.

Besides, since input signals usually have DC offsets, improvements on the SNR performance of the proposed system over the

conventional system and the system with an additive dithering for input signals with DC offsets are shown in Fig. 14. Similar to the above, an additive white noise source with a uniform distribution between  $[-1, 1]$  is added and subtracted before and after the quantizer in the system with an additive dithering, respectively. Now, we assume that there is a small DC offset in the input signal. That is,  $u(k) = 0.01 + U \sin(\frac{2\pi k}{3R})$  for  $k \geq 0$ . Same as the above,  $R = 64$  and  $U$  is the magnitude of the sinusoidal input. The quantizer is assumed to be a single bit antisymmetric one with the saturation level equal to one. That is,

$$Q'(y) \equiv \begin{cases} 1 & y \geq 0, \\ -1 & \text{otherwise,} \end{cases}$$

and  $L = 1$ . The periodic codes employed in these numerical computer simulations consist of 40 coefficients with  $M = 10$ . According to the numerical computer simulation results, the proposed system

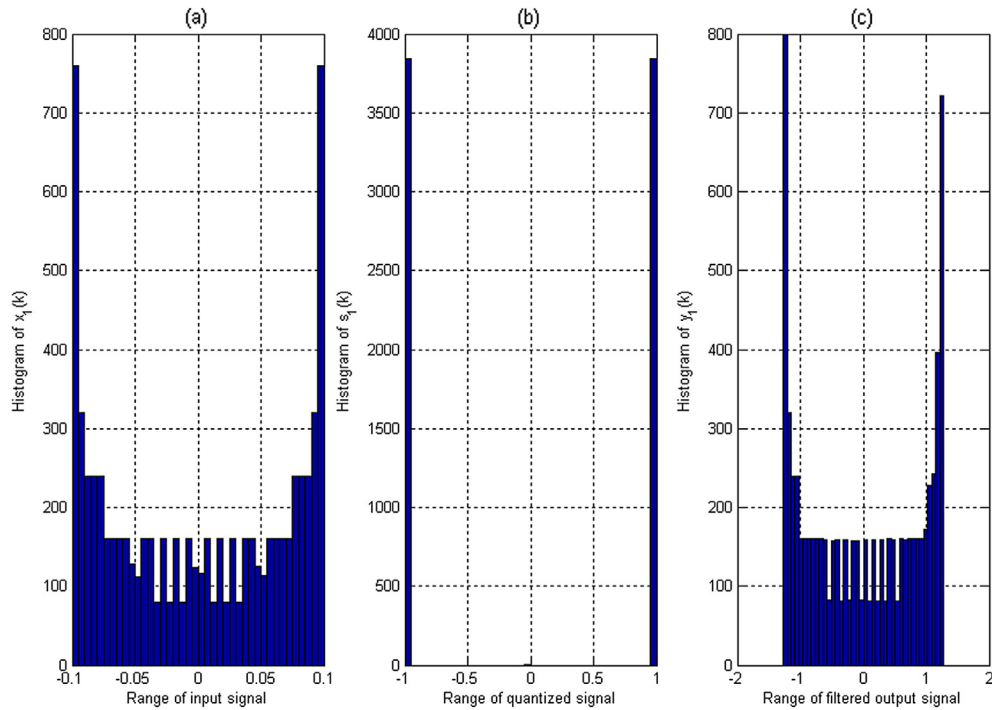


Fig. 16. Histograms of the input signal, the quantized signal and the output of the conventional system.

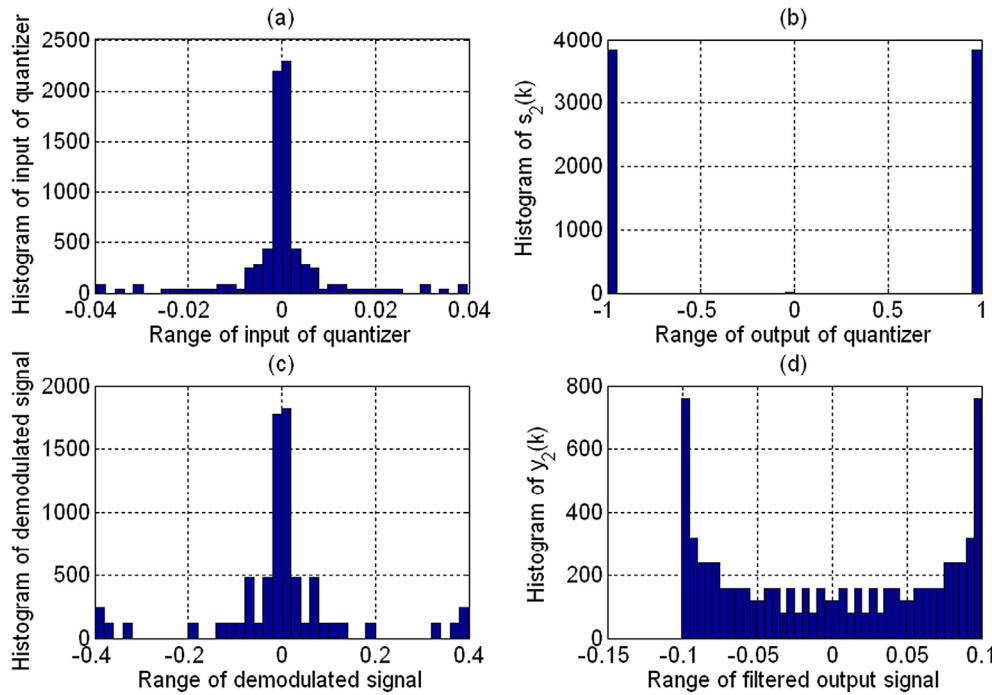


Fig. 17. Histograms of the input of the quantizer, the output of the quantizer, the demodulated signal and the output of the proposed system.

could achieve an average of 52.2884 dB improvement over the conventional system and an average of 36.1280 dB improvement over the system with an additive dithering. Although there are drops in terms of the improvements, the proposed system still achieves very significant improvements over the system with an additive dithering and the conventional system when there is a DC offset in the input signal.

In addition, since the periodic code is usually stored in memory and it is represented using a finite length, improvements on

the SNR performance of the proposed system over the conventional system and the system with an additive dithering when the periodic code is represented using an 8 bits length are shown in Fig. 15. 8 bits are used here because they are usually enough for representing most signals. Similar to the above, an additive white noise source with a uniform distribution between  $[-1, 1]$  is added and subtracted before and after the quantizer in the system with an additive dithering, respectively. The input signal is  $u(k) = U \sin(\frac{2\pi k}{3R})$  for  $k \geq 0$ . Same as the above,  $R = 64$  and  $U$  is

the magnitude of the sinusoidal input. The quantizer is assumed to be a single bit antisymmetric one with the saturation level equal to one. That is,

$$Q'(y) \equiv \begin{cases} 1 & y \geq 0, \\ -1 & \text{otherwise,} \end{cases}$$

and  $L = 1$ . The periodic codes employed in these numerical computer simulations consist of 40 coefficients with  $M = 10$ , but they are represented using an 8 bit length. According to the numerical computer simulation results, the proposed system could achieve an average of 57.3593 dB improvement over the conventional system and an average of 41.1132 dB improvement over the system with an additive dithering. Although there are drops in terms of the improvements, the proposed system still achieves very significant improvements over the system with an additive dithering and the conventional system when the periodic code is represented using a finite length.

To understand more why the proposed system can achieve such significant improvements, Fig. 16 shows the histograms of the input signal, the quantized signal and the output of the conventional system when a single bit antisymmetric quantizer with the saturation level equal to one, that is

$$Q'(y) \equiv \begin{cases} 1 & y \geq 0, \\ -1 & \text{otherwise,} \end{cases}$$

is employed. Same as the above, the input signal  $u(k) = U \sin(\frac{2\pi k}{3R})$  for  $k \geq 0$ , where  $R = 64$  and  $U = 0.1$ . Fig. 17 shows the histograms of the input of the quantizer, the output of the quantizer, the demodulated signal and the output of the proposed system with 40 coefficients. Here,  $M = 10$ . 40 coefficients with  $M = 10$  is employed because of the similar reasons discussed in the above. It can be seen from Fig. 16 that the dynamical range of the output of the conventional system is between  $-1.27$  and  $1.27$ , which is about 1200% of that of the input signal. Hence, the SNR ratio is low. On the other hand, it can be seen from Fig. 17 that the dynamical range of the output of the proposed system has the same dynamical range as that of the input signal. Hence, the proposed system achieves higher SNR compared to the conventional one.

## 6. Conclusions

In this paper, a quantization model is proposed. The proposed model is different from the conventional one because the conventional one models the quantizer as an additive white noise source, while the proposed one models the quantizer as a high order nonlinear memoryless system. A periodic code is multiplied to both the input and output of the quantizer for reducing the quantization noise. The condition for an improvement on the SNR is derived. Moreover, an optimal periodic code is designed via a modified gradient descent method. Numerical computer simulation results show that there are significant improvements on the SNR performances compared to existing systems such as the conventional system without multiplying to the periodic code, the system with an additive dithering and a first order sigma delta modulator. Besides, the instability issue occurred in the sigma delta modulation approach does not occur in the proposed system.

## Acknowledgments

This paper was supported partly by the National Nature Science Foundation of China (No. 61372173), the Doctoral Fund of Ministry of Education of China (No. 20110171120044), the Guangdong Higher Education International Cooperative Item “Facing the Application of Manufacturing of the Internet of Things: Construction and Optimization Decision Methods of Real-time Information Networks

(ghzh1005)”, the Hundred People Plan from the Guangdong University of Technology and the Young Thousand People Plan from the Ministry of Education of China.

## References

- [1] E.H. Yang, Z. Zhang, An on-line universal lossy data compression algorithm via continuous codebook refinement—part III: redundancy analysis, *IEEE Trans. Inform. Theory* 44 (5) (1998) 1782–1801.
- [2] D.E. Quevedo, G.C. Goodwin, Multistep optimal analog-to-digital conversion, *IEEE Trans. Circuits Syst. I. Regul. Pap.* 52 (3) (2005) 503–515.
- [3] N.T. Thao, Vector quantization analysis of  $\Sigma\Delta$  modulation, *IEEE Trans. Signal Process.* 44 (4) (1996) 808–817.
- [4] M.G. Strintzis, D. Tzovaras, Optimal pyramidal decomposition for progressive multidimensional signal coding using optimal quantizers, *IEEE Trans. Signal Process.* 46 (4) (1998) 1054–1068.
- [5] C.Y.F. Ho, B.W.K. Ling, J.D. Reiss, X. Yu, Nonlinear behaviors of bandpass sigma delta modulators with stable system matrices, *IEEE Trans. Circuits Syst., II Express Briefs* 53 (11) (2006) 1240–1244.
- [6] C.Y.F. Ho, B.W.K. Ling, J.D. Reiss, Fuzzy impulsive control of high order interpolative lowpass sigma delta modulators, *IEEE Trans. Circuits Syst. I. Regul. Pap.* 53 (10) (2006) 2224–2233.
- [7] C.Y.F. Ho, B.W.K. Ling, J.D. Reiss, Y.Q. Liu, K.L. Teo, Design of interpolative sigma delta modulators via semi-infinite programming, *IEEE Trans. Signal Process.* 54 (10) (2006) 4047–4051.
- [8] Z. Cvetković, M. Vetterli, On simple oversampled A/D conversion in  $L^2(\mathbb{R})$ , *IEEE Trans. Inform. Theory* 47 (1) (2001) 146–154.
- [9] M.S. Iyer, R.R. Rhinehart, A method to determine the required number of neural-network training repetitions, *IEEE Trans. Neural Netw.* 10 (2) (1999) 427–432.
- [10] N.T. Thao, S. Güntürk, Generalized spectral theory for  $\Sigma\Delta$  quantization with constant inputs, in: *International Conference on Acoustics, Speech and Signal Processing, ICASSP*, vol. III, 2006, pp. 540–543.
- [11] C.Y.F. Ho, J.D. Reiss, B.W.K. Ling, Using SIP techniques to verify the trade-off between SNR and information capacity of a sigma delta modulator, in: *Audio Engineering Society 120th Convention*, 2006, Paper Number 6697.
- [12] G.D. Altinok, M. Al-Janabi, I. Kale, Stability analysis of bandpass sigma-delta modulators for single and dual tone sinusoidal inputs, *IEEE Trans. Instrum. Meas.* 60 (5) (2011) 1546–1554.
- [13] J. Lota Al-Janabi, I. Kale, Nonlinear-stability analysis of higher order  $\Delta-\Sigma$  modulators for DC and sinusoidal inputs, *IEEE Trans. Instrum. Meas.* 57 (3) (2008) 530–542.
- [14] M. Nagahara, Y. Yamamoto, Frequency domain min-max optimization of noise-shaping delta-sigma modulators, *IEEE Trans. Signal Process.* 60 (6) (2012) 2828–2839.



**Bingo Wing-Kuen Ling** received the B.Eng. (Hons) and M.Phil. degrees from the department of Electronic and Computer Engineering, the Hong Kong University of Science and Technology, in 1997 and 2000, respectively, and the Ph.D. degree in the department of Electronic and Information Engineering from the Hong Kong Polytechnic University, in 2003. In 2004, he joined the King's College London as a Lecturer. In 2010, he joined the University of Lincoln as a Principal Lecturer and promoted to a Reader, in 2011. In 2012, he joined the Guangdong University of Technology as a Full Professor. He is a Fellow of IET, a senior member of IEEE, a China National Young Thousand-People-Plan Distinguished Professor and University Hundred-People-Plan Distinguished Professor. He serves in the technical committees of the nonlinear circuits and systems group, the digital signal processing group and the power electronics and systems group of the IEEE Circuits and Systems Community. He was awarded the best reviewer prizes from the IEEE Instrumentation and Measurement Society, in 2008 and 2012. He has also served as the guest editor-in-chief of several special issues of highly rated international journals, such as the *Circuits, Systems and Signal Processing*, and the *American Journal of Engineering and Applied Sciences*, and is currently an associate editor of the *International Journal of Bifurcation and Chaos*, and the *Circuits, Systems and Signal Processing*, etc. He has published an undergraduate textbook, a research monograph, several book chapters, a book review published in an IEEE journal, more than 75 internationally leading journal papers and more than 55 highly rated international conference papers. He has held 7 visiting positions and delivered more than 20 seminars in the field of image processing, time frequency analysis, optimization theory, symbolic dynamics as well as fuzzy and impulsive control theory.



**Charlotte Yuk-Fan Ho** received the B.Eng. (Hons) degree from the department of Electronic and Computer Engineering, the Hong Kong University of Science and Technology, in 2000, and the MPhil. Degree from the department of Electronic and Information Engineering, the Hong Kong Polytechnic University, in 2003. She is pursuing her Ph.D. study at the Queen Mary, University of London. Her research interests include image processing, filter banks and wavelets theory, functional inequality constrained optimization problems, symbolic dynamics as well as fuzzy and impulsive control theory.



**Joshua D. Reiss** received his bachelor degrees in both physics and mathematics and Ph.D. degree in physics from the Georgia Institute of Technology. In 2000, he accepted a research position in the Audio Signal Processing research laboratory at King's College London. Then, he moved to Queen Mary University of London, in 2001. He is currently a senior lecturer. His research focus includes chaotic time series and audio engineering.



**Qingyun Dai** received her Ph.D. degree in South China University of Technology. She is a Full Professor in the School of Information Engineering, the Director of Intelligent Signal Processing and Big Data Research Center and the Director of Science and Technology Research Office of the Guangdong University of Technology. Her research interests mainly include wavelets, image processing, image retrieval, pattern recognition, manufacturing engineering systems, RFID, cloud computing and big data, etc.